

$KN\Lambda$ and $KN\Sigma$ coupling constants from the Chiral Bag Model

M.T. Jeong¹, Il-T. Cheon²¹ Department of Physics, Dongshin University, Naju 520-714, Korea (e-mail: mjeong@dongshinu.ac.kr)² Department of Physics, Yonsei University, Seoul 120-749, Korea (e-mail: itcheon@phy.yonsei.ac.kr)

Received: 17 August 1998 / Revised version: 22 December 1998

Communicated by F. Lenz

Abstract. The $KN\Lambda$ and $KN\Sigma$ coupling constants have been calculated in the framework of the Chiral Bag Model (CBM). We find $-3.88 \leq g_{KN\Lambda} \leq -3.67$ and $1.15 \leq g_{KN\Sigma} \leq 1.24$ by taking into account pseudoscalar mesons (π, K) and vector mesons (ρ, ω, K^*) field effects. Particularly, it is shown that vector mesons make significant contributions to the coupling constants $g_{KN\Lambda}$ and $g_{KN\Sigma}$. Our values are existing within the experimental limits compared to the phenomenological values extracted from the kaon photoproduction and kaon-nucleon scattering experiments. Also, form factors are suggested for the πNN , $\pi N\Delta$, $KN\Lambda$ and $KN\Sigma$ couplings.

PACS. 13.75.Jz Kaon-baryon interactions – 14.40.Aq π, k , and η mesons

1 Introduction

The kaon physics has been consistently investigated in the intermediate energy nuclear physics, which ranges from simple processes like the kaon-nucleon scattering or the kaon photoproduction on a nucleon to the spectroscopy and structure of hypernuclei. The most fundamental coupling constants in the kaon-nucleon physics are the $KN\Lambda$ and $KN\Sigma$ coupling constants. The extraction of precise values for $g_{KN\Lambda}$ and $g_{KN\Sigma}$ is not yet allowed due to the limited set of data, while the πNN coupling constant $g_{\pi NN}$ is determined accurately through either the nucleon-nucleon scattering or the pion-nucleon scattering experiment. Over the years, most analyses of the kaon photoproduction on a nucleon have focused on the two processes $\gamma p \rightarrow K^+\Lambda$ and $\gamma p \rightarrow K^+\Sigma^0$. There have been many attempts to determine the coupling constants $g_{KN\Lambda}$ and $g_{KN\Sigma}$ from these kaon photoproduction [1–5]. Within a phenomenological approach, Adelseck et al. [2,3] extracted the coupling constants by performing a least-squares search similar to that of Thom's [4]. However, these results turned out to have large uncertainties, $-1.29 \geq g_{KN\Lambda}/\sqrt{4\pi} \geq -4.17$, due to the simultaneous determination of many other unknown coupling constants. Also, to theoretically reproduce the experimental kaon-nucleon scattering cross-section, one usually calculates the contributions from the one-boson exchanges, the resonances in the s-channel, such as the Λ and Σ , and the next to leading two meson exchanges [1]. These involve many phenomenologically undetermined coupling constants so that it seems a formidable task to determine the coupling constants related to the kaon separately. Therefore, it is necessary to explore theoretical predictions because of un-

certainties and difficulties in extracting the precise values for these coupling constants from the experiments.

At present, the quantum chromodynamics (QCD) is believed to be the basic theory of the strong interaction. The MIT bag model [6], soliton model [7], and skyrme model [8] are amongst the best known phenomenological models of QCD. Deriving from QCD, by functional-integral methods, the phenomenological models of hadrons, Cahill et. al [9] showed that all sorts of meson-quarks interactions, e.g., the interactions with π, ρ, ω , etc., are self-contained in the theory. The chiral soliton [10–12] and chiral bag models [13,14] which have been studied by many groups are based on the σ model. The soliton or bag excitations provide the baryons, whose masses are in the GeV range. Therefore, it seems reasonable to include in the theory also vector mesons, like the ω, ρ and K^* , whose masses are lower than the masses of the baryons. The interesting outcome is that the introduction of vector mesons by itself stabilizes the chiral soliton [15] and chiral bag [16] models. Also, there are some arguments that the quartic term in the Skyrme model represents the degree of freedoms of the ω -meson [15].

Araki [17] calculated the values of $g_A, g_{\pi NN}$ and μ_N in the framework of the nonlinear chiral soliton model. As a result, they showed that it gave too a large g_A and too small nucleon magnetic moments, and the introduction of the ω -quark interaction was able to give an overall agreement of $g_A, g_{\pi NN}$ and μ_N . Recent calculations in the chiral bag model (CBM) provided somewhat reasonable descriptions of the nucleon electromagnetic (e.m.) form factors [18]. However, these results show an irreconcilability between the proton magnetic and electric form factors; i.e., better results for the magnetic form factors induce

less satisfactory results for the electric form factors. The CBM with vector mesons (CBMVM) improves remarkably the theoretical curves of nucleon form factors as well as the values of nucleon magnetic moments and nucleon e.m. radii [19]. Also, Theberge et al. [14] calculated the magnetic moments for all members of the $J^P = (1/2)^+$ octet baryons ($n, p, \Sigma^\pm, \Lambda, \Xi^{-,0}$) including the strange baryons in the framework of the CBM, and they showed excellent agreement with data within the 10% level. Therefore, one can make use of the CBM to analyze the hyperons (Σ, Λ).

The aim of this paper is to calculate the coupling constants $g_{KN\Lambda}$ and $g_{KN\Sigma}$ in the framework of the CBMVM. We analyze the hadronic πNN coupling constant at first, and then, we calculate $g_{KN\Lambda}$ and $g_{KN\Sigma}$ using extension from SU(2) CBMVM to the SU(3) and taking into account the vector mesons (ρ, ω, K^*) as well as the pseudoscalar mesons (π, K). The quark-meson coupling constants are determined by fitting the renormalized πNN coupling constant. Our predictions are compared with the values extracted from phenomenological analyses and other theoretical QCD calculations. Also, form factors are suggested for πNN , $\pi N\Delta$, $KN\Lambda$ and $KN\Sigma$.

2 Interaction lagrangians containing vector mesons

The Lagrangian containing vector mesons can be derived by a local gauge transformation of the CBM Lagrangian given by Kalbermann and Eisenberg [13], i.e. ρ -mesons are coupled to the SU(2) isospin and ω -mesons are coupled to the U(1) baryon number. Therefore, the minimal coupling

$$\partial_\mu \longrightarrow \partial_\mu - \frac{i}{2}g_v(\boldsymbol{\tau} \cdot \boldsymbol{\rho}_\mu + \omega_\mu) \quad (1)$$

induces the effective Lagrangian

$$\begin{aligned} \mathcal{L} = & \bar{q}i\gamma^\mu \left(\partial_\mu - \frac{i}{2}g_v\boldsymbol{\tau} \cdot \boldsymbol{\rho}_\mu - \frac{i}{2}g_v\omega_\mu \right) q\Theta_V - B\Theta_V - \frac{1}{2}\bar{q}q\Delta_S \\ & + \bar{q}\gamma^\mu \frac{1}{1+g_\pi^2\pi^2} [g_\pi\gamma_5\boldsymbol{\tau} \cdot D_\mu\boldsymbol{\pi} - g_\pi^2\boldsymbol{\tau} \cdot (\boldsymbol{\pi} \times D_\mu\boldsymbol{\pi})] q\Theta_V \\ & + \frac{1}{2} \frac{1}{(1+g_\pi^2\pi^2)^2} D^\mu\boldsymbol{\pi} \cdot D_\mu\boldsymbol{\pi} \\ & - \frac{1}{2} \frac{1}{(1+g_\pi^2\pi^2)} m_\pi^2\boldsymbol{\pi}^2 - \frac{1}{4}\boldsymbol{\rho}^{\mu\nu} \cdot \boldsymbol{\rho}_{\mu\nu} + \frac{1}{2}m_\rho^2\boldsymbol{\rho}^\mu \cdot \boldsymbol{\rho}_\mu \\ & - \frac{1}{4}\omega^{\mu\nu}\omega_{\mu\nu} + \frac{1}{2}m_\omega^2\omega^\mu\omega_\mu \\ & + \frac{3g_\pi g_v^2}{4\pi^2} \varepsilon^{\mu\nu\alpha\beta} \partial_\mu\omega_\nu\boldsymbol{\rho}_\alpha \cdot \partial_\beta\boldsymbol{\pi}, \end{aligned} \quad (2)$$

where

$$\begin{aligned} \boldsymbol{\rho}_{\mu\nu} &= \partial_\mu\boldsymbol{\rho}_\nu - \partial_\nu\boldsymbol{\rho}_\mu + g_v\boldsymbol{\rho}_\mu \times \boldsymbol{\rho}_\nu, \\ \omega_{\mu\nu} &= \partial_\mu\omega_\nu - \partial_\nu\omega_\mu, \\ D_\mu\boldsymbol{\pi} &= \partial_\mu\boldsymbol{\pi} + g_v\boldsymbol{\rho}_\mu \times \boldsymbol{\pi}. \end{aligned} \quad (3)$$

B is the vacuum energy constant, D_μ is the covariant derivative, $g_\pi = 1/2f_\pi$ with the pion decay constant f_π ,

and $q(x)$ and $\pi(x)$ are quark and pion fields, respectively. Θ_V and Δ_S denote the volume and surface δ functions. The last term in Eq. (2) is the so-called Wess-Zumino term [20], which describes a certain anomaly processes containing π , ρ and ω . With this effective Lagrangian Eq. (2), one can derive the interactions of the pion-quark and vector meson-quark as

$$\mathcal{L}_{\pi qq} = g_\pi \int d^3x \bar{q}(x)\gamma^\mu\gamma_5\boldsymbol{\tau} \cdot D_\mu\boldsymbol{\pi}(x)q(x)\Theta_V, \quad (4)$$

$$\mathcal{L}_{vqq} = g_v \int d^3x \bar{q}(x)\gamma^\mu[\boldsymbol{\tau} \cdot \boldsymbol{\rho}_\mu(x) + \omega_\mu(x)]q(x)\Theta_V. \quad (5)$$

The gauge coupling constant g_v in Eq.(5) can be evaluated by the $\rho \rightarrow 2\pi$ or $\omega \rightarrow \pi\gamma$ decay processes, and satisfies the well known Kawarabayashi-Suzuki-Riazuddin-Fayyazuddin (KSRF) relation [21]. In general, the coupling constant prefers the range of $4 \leq g_v \leq 6$ [22].

3 The πNB ($B = N, \Delta$) form factors

The πNN and $\pi N\Delta$ form factors can be obtained by evaluating the Feynman diagrams shown in Fig. 1 with Lagrangians (4), (5) and the Wess-Zumino term. The form factor $g_{\pi NB}(k_\pi)$ associated with each diagram is given as

$$\begin{aligned} \frac{g_{\pi NB}(k_\pi^r)}{2M} = & Ag_\pi U(k_\pi^r) + \frac{g_\pi}{144\pi^2} \sum_{SS'} \\ & \left\{ g_\pi^2 U(k_\pi^r) \int dk_\pi k_\pi^4 \frac{B_{SS'} U^2(k_\pi)}{\omega_\pi(\omega_\pi + \omega_{NS})(\omega_\pi + \omega_\pi^r + \omega_{NS'})} \right. \\ & + g_v^2 U(k_\pi^r) \int dk_v k_v^2 \left(\frac{C_{SS'} S_1^2(k_v)}{\omega_v(\omega_v + \omega_{NS})(\omega_v + \omega_\pi^r + \omega_{NS'})} \right. \\ & \left. \left. + \frac{D_{SS'} S_0^2(k_v)}{\omega_v^2(\omega_v + \omega_\pi^r)} \right) \right. \\ & + g_\pi g_v \int dk_\pi (\mathbf{k}_\pi \cdot \mathbf{k}'_v) U(k_\pi) \\ & \times \left(\frac{E_S S_1(k'_v)}{(\omega_\pi + \omega'_v)(\omega_\pi + \omega_{NS})(\omega'_v + \omega_{NS})} + \frac{F_S S_0(k'_v)}{\omega_\pi^2 \omega_v'^2} \right) \\ & + \frac{9g_v^4}{4\pi^2} \int dk_v k_v \frac{(\mathbf{k}_v \times \mathbf{k}'_v)(\omega_v + \omega'_v + \omega_{NS})}{\omega_v \omega'_v (\omega_v + \omega_{NS})(\omega'_v + \omega_{NS})(\omega_v + \omega'_v)} \\ & \left. \times [G_S S_0(k'_v) S_1(k_v) + H_S S_0(k_v) S_1(k'_v)] \right\} \end{aligned} \quad (6)$$

where k_π^r and ω_π^r are the real pion momentum and energy, k_π and ω_π are the virtual pion momentum and energy, $\mathbf{k}'_v = \mathbf{k}_v + \mathbf{k}_\pi^r$ and $\omega'_v = \sqrt{m_v^2 + k_v'^2}$, and $\omega_{NS} = m_S - m_N$. The suffixes S and S' denote N or Δ . We have also introduced vertex functions in the forms of

$$U(k) = N^2 \int_0^R r^2 dr \left(j_0(kr) [j_0^2(\Omega r/R) - \frac{1}{3}j_1^2(\Omega r/R)] - j_2(kr) j_1^2(\Omega r/R) \right) \quad (7)$$

$$S_0(k_v) = \frac{1}{2} N^2 \int_0^R r^2 dr [j_0^2(\Omega r/R) + j_1^2(\Omega r/R)] j_0(k_v r), \quad (8)$$

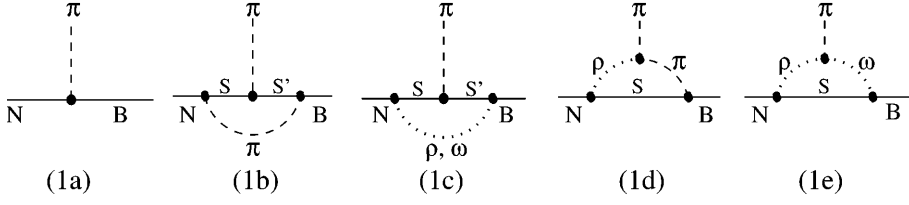


Fig. 1. Feynman diagrams for the πNN and $\pi N\Delta$ form factors

$$S_1(k_v) = \frac{5}{3} N^2 \int_0^R r^3 dr j_0(\Omega r/R) j_1(\Omega r/R) j_1(k_v r). \quad (9)$$

Here, $\Omega = 2.043$ is obtained by the bag boundary condition, $j_0(\Omega) = j_1(\Omega)$. Coefficients in Eq.(6) are given by $A = 5/3(2\sqrt{2})$, $B_{NN} = 250(800\sqrt{2})$, $B_{N\Delta} = 1280(64\sqrt{2})$, $B_{\Delta N} = 1280(1000\sqrt{2})$, $B_{\Delta\Delta} = 1280(800\sqrt{2})$, $C_{NN} = 295(1088\sqrt{2})$, $C_{\Delta N} = 1280(64\sqrt{2})$, $C_{N\Delta} = 1280(1000\sqrt{2})$, $C_{\Delta\Delta} = 1600(800\sqrt{2})$, $D_{NN} = -180(200\sqrt{2})$, $E_N = 100(60\sqrt{2})$, $E_\Delta = 32(30\sqrt{2})$, $F_N = 160(100\sqrt{2})$, $G_N = -64(-32\sqrt{2})$, $G_\Delta = 320(-24\sqrt{2})$, $H_N = 128(0)$ and $H_\Delta = 0(30\sqrt{2})$ for the $\pi NN(\pi N\Delta)$ form factors.

The πNN coupling constant is determined by the values of the πNN form factors at $k_\pi^r = 0$. The result of numerical calculation for Eq.(6) at $k_\pi^r = 0$ is expressed by

$$\frac{[g_{\pi NN}(0)]^2}{4\pi} = g_{\pi q}^2 \left[4.154 + 0.630g_{\pi q}^2 + 0.00641g_v^2 + 0.00933g_{\pi q}g_v + 0.00044g_v^4 \right]^2. \quad (10)$$

The numerical values of each term have been calculated with $R = 0.90 fm$. The renormalized πNN coupling constant $[g_{\pi NN}(0)]^2/4\pi = 14.3$ can be obtained by substituting the vqq coupling constant $g_v = 5.21$ and the πqq dimensionless coupling constant $g_{\pi q} = m_{\pi^+}/(2f_\pi)$ with the experimental value of the pion decay constant $f_\pi = 93 MeV$. The last term of Eq.(6) denotes the Wess-Zumino term in Fig. (1e) and the coupling constant $g_{\pi\rho\omega} = 3g_\pi g_v^2/4\pi^2$ can be evaluated by the $\omega \rightarrow \pi\gamma$ decay width. Using the current-field identity and the limit of vector meson dominance, we obtain $g_{\omega\pi\gamma}/m_\pi = 3g_\pi g_v e/4\pi^2 = 0.306e/m_\pi$, which is a little small compared with $g_{\omega\pi\gamma} = (0.373 \pm 0.018)e$ deduced from the $\omega \rightarrow \pi\gamma$ decay width ($\Gamma = 0.89 MeV$). Calculating the first order diagram of Fig. (1a) with these coupling constants, we find the bare πNN coupling constant $[g_{\pi NN}(0)]^2/4\pi = 9.70$. Calculating the Feynman diagrams of the Figs.(1a) and (1b), we find $[g_{\pi NN}(0)]^2/4\pi = 11.4$, which corresponds to the result obtained without vector mesons. The renormalized πNN coupling constant $[g_{\pi NN}(0)]^2/4\pi = 14.3$ is obtained by including vector meson effects of Figs.(1c) \sim (1e). Calculating the Feynman diagrams of Figs.(1a), (1a \sim 1b) and (1a \sim 1e), we obtain the $\pi N\Delta$ coupling constant $G_3 = g_{\pi N\Delta}(0)/2M = 1.41/m_\pi$, $1.65/m_\pi$ and $2.01/m_\pi$, respectively. Here, the last value, $G_3 = 2.01/m_\pi$, reproduces the $\Delta\pi N$ decay width $\Gamma = 122 MeV$, which is a little larger compared with the measured decay width $\Gamma = 115 \pm 5 MeV$. However, the $\pi N\Delta$ coupling constant is a little smaller compared with the $\pi N\Delta$ coupling

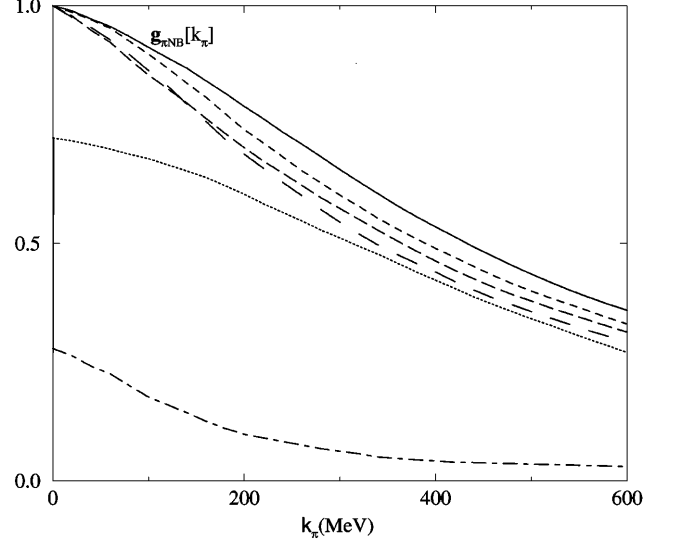


Fig. 2. The renormalized πNN and $\pi N\Delta$ form factors. The solid and dashed curves are the numerical results of the πNN and $\pi N\Delta$ form factors, respectively, where we use the bag radius $R = 0.90 fm$. The dotted curve represents quark contribution from diagrams (1a), (1b) and (1c) for the $\pi N\Delta$ form factor. The dot-dashed curve shows meson contribution from diagrams (1d) and (1e) for the $\pi N\Delta$ form factor. The short dashed and long dashed curves denote the πNN and $\pi N\Delta$ form factors, respectively, resulting from model(2) of ref. [25]

constant of the BL amplitude [23], $G_3 = 2.18/m_\pi$, which is determined by fitting the process, $p(\gamma, \pi^+)n$.

The numerical results of the πNN and $\pi N\Delta$ form factors with $R = 0.90 fm$ are shown in Fig. 2. The solid and dashed curves are the numerical results of the πNN and $\pi N\Delta$ form factors, respectively. The dotted curve represents quark contribution from diagrams (1a), (1b) and (1c) for the $\pi N\Delta$ form factor. The dot-dashed curve shows meson contribution from diagrams (1d) and (1e) for the $\pi N\Delta$ form factor. We can see that the $\pi N\Delta$ form factor falls down a little faster than the πNN form factor. The reason is that meson contributions to $\pi N\Delta$ coupling are considerably large compared with those to πNN coupling, where the meson contributions fall down gradually faster than quark contributions as the momentum transfer increases.

Our πNN and $\pi N\Delta$ form factors are less soft than those determined from a microscopic model for πN scattering [24,25]. The short dashed and long dashed curves denote the πNN and $\pi N\Delta$ form factors, respectively, resulting from model(2) of ref. [25]. The recent experiments [26] for the reactions $\nu_\mu + n \rightarrow \mu^- + p$ and

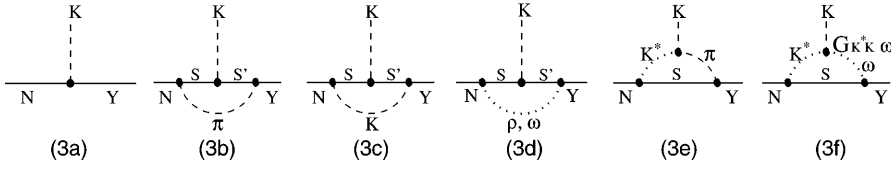


Fig. 3. Feynman diagrams for the KNA and $KN\Sigma$ form factors

$\nu_\mu + p \rightarrow \mu^- + \Delta^{++}$ can provide empirical information for the πNN and $\pi N\Delta$ form factors. Our πNN and $\pi N\Delta$ form factors are softer than the axial NN and $N\Delta$ transition form factors obtained by the Kitagaki et. al [26], respectively.

4 The KNY ($Y = \Lambda, \Sigma$) form factors

The $KNA(\Sigma)$ coupling constant can be calculated by extending from the basic doublet (u, d) to a triplet (u, d, s), substituting the λ_i of $SU(3)$ generators for the τ_i of $SU(2)$, and taking into account pseudoscalar mesons (π, K) and vector mesons (ω, ρ, K^*). Therefore, Kqq and K^*qq interactions are expressed by

$$\mathcal{L}_{Kqq} = g_k \int d^3x \bar{q}(x) \gamma^\mu \gamma_5 \boldsymbol{\lambda} \cdot D_\mu \mathbf{K}(x) q(x) \Theta_V, \quad (11)$$

$$\mathcal{L}_{K^*qq} = g_v^* \int d^3x \bar{q}(x) \gamma^\mu \boldsymbol{\lambda} \cdot \mathbf{K}_\mu^*(x) q(x) \Theta_V. \quad (12)$$

The $KNA(\Sigma)$ form factor can be obtained by calculating the Feynman diagrams shown in Fig. 3 with Lagrangians (4), (5), (11), (12) and the Wess-Zumino term. The form factor $g_{KNY}(k_k^r)$ associated with each diagram is given as

$$\begin{aligned} \frac{g_{KNY}(k_k^r)}{2M} &= Ag_k U(k_k^r) + \frac{g_k}{144\pi^2} \sum_{SS'} \\ &\left\{ g_\pi^2 U(k_k^r) \int dk_\pi \frac{B_{SS'} k_\pi^4 U^2(k_\pi)}{\omega_\pi (\omega_\pi + \omega_{NS}) (\omega_\pi + \omega_k^r + \omega_{NS'})} \right. \\ &+ g_k^2 U(k_k^r) \int dk_k \frac{C_{SS'} k_k^4 U^2(k_k)}{\omega_k (\omega_k + \omega_{NS}) (\omega_k + \omega_k^r + \omega_{NS'})} \\ &+ g_v^2 \int dk_v k_v^2 U(k_v^r) \left(\frac{D_{SS'} S_1^2(k_v)}{\omega_v (\omega_v + \omega_{NS}) (\omega_v + \omega_k^r + \omega_{NS'})} \right. \\ &\quad \left. + \frac{E_{SS'} S_0^2(k_v)}{\omega_v^2 (\omega_v + \omega_k^r)} \right) \\ &+ g_\pi g_v^* \int dk_\pi (\mathbf{k}_\pi \cdot \mathbf{k}_v^*) U(k_\pi) \\ &\quad \times \left(\frac{F_S S_1(k_v^*)}{(\omega_\pi + \omega_v^*) (\omega_\pi + \omega_{NS}) (\omega_v^* + \omega_{NS})} + \frac{G_S S_0(k_v^*)}{\omega_\pi^2 \omega_v^{*2}} \right) \\ &+ \frac{9g_v^2 g_v^{*2}}{4\pi^2} \int dk_v k_v \frac{(\mathbf{k}_v \times \mathbf{k}_v^*) (\omega_v + \omega_v^* + \omega_{NS})}{\omega_v \omega_v^* (\omega_v + \omega_{NS}) (\omega_v^* + \omega_{NS}) (\omega_v + \omega_v^*)} \\ &\quad \left. \times [H_S S_1(k_v^*) S_0(k_v) + I_S S_1(k_v) S_0(k_v^*)] \right\}, \quad (13) \end{aligned}$$

where $\mathbf{k}_v^* = \mathbf{k}_v + \mathbf{k}_k^r$, $\omega_v^* = \sqrt{m_v^2 + k_v^{*2}}$ and $g_k = 1/(2f_k)$ with the experimental value of the kaon decay constant

$f_k = 114 \text{ MeV}$. The hadronic coupling constant, $g_v^* = g_v$, can be inferred from the $SU(3)$ symmetry assumption. The suffixes S and S' denote N, Λ and Σ having strangeness 0 or -1 for the octet with $J^P = \frac{1}{2}^+$, and Δ and Σ^* having strangeness 0 or -1 for the decuplet with $J^P = \frac{3}{2}^+$. Their $SU(3)$ wave functions of three quarks can be found in [27]. Coefficients in (13) are given by $A = -\sqrt{3}(1/3)$, $B_{N\Lambda} = -125\sqrt{3}(100)$, $B_{N\Sigma} = -640\sqrt{3}(500)$, $B_{N\Sigma^*} = -160\sqrt{3}(250)$, $B_{\Delta\Sigma} = -128\sqrt{3}(76)$, $B_{\Delta\Sigma^*} = -256\sqrt{3}(76)$, $C_{N\Lambda} = -525\sqrt{3}(270)$, $C_{N\Sigma} = -1050\sqrt{3}(60)$, $C_{N\Sigma^*} = -210\sqrt{3}(24)$, $C_{\Delta\Sigma} = -64\sqrt{3}(36)$, $C_{\Delta\Sigma^*} = -256\sqrt{3}(72)$, $D_{N\Lambda} = -125\sqrt{3}(100)$, $D_{N\Sigma} = -640\sqrt{3}(500)$, $D_{N\Sigma^*} = -160\sqrt{3}(250)$, $D_{\Delta\Sigma} = -128\sqrt{3}(76)$, $D_{\Delta\Sigma^*} = -256\sqrt{3}(76)$, $E_{N\Lambda} = -540\sqrt{3}(0)$, $E_{N\Sigma} = 0(180)$, $F_N = -160\sqrt{3}(40)$, $F_\Delta = -60\sqrt{3}(20)$, $G_\Lambda = -64\sqrt{3}(12)$, $G_\Sigma = -108\sqrt{3}(32)$, $G_{\Sigma^*} = -48\sqrt{3}(-16)$, $H_N = -320\sqrt{3}(-24)$, $I_\Lambda = -128\sqrt{3}(0)$ and $I_\Sigma = 0(216)$ for the $KNA(KN\Sigma)$ form factors. The last term in (13) denotes the Wess-Zumino term shown in Fig. 3f, and the $K^*K\omega$ coupling constant can be evaluated by the $K^* \rightarrow K\gamma$ decay width. Our value, $G_{K^*K\omega}/m_k = 3g_k g_v^* g_v / (4\pi^2)$, induces $G_{K^*K\gamma}/m_k = 3g_k g_v^* e / (4\pi^2) = 0.859e/m_k$ by the current-field identity [22] and the limit of vector meson dominance. The relation [4] of the $K^*K\gamma$ coupling constant to the decay width provides $\Gamma_{K^* \rightarrow K\gamma} = \frac{9.8 \text{ MeV}}{4\pi} |G_{K^*K\gamma}|^2 = 53 \text{ MeV}$ [28], which is within the measured decay width $50 \pm 5 \text{ MeV}$.

Substituting the $f_\pi = 93 \text{ MeV}$, $f_k = 114 \text{ MeV}$, $g_v = 5.21$ and $R = 0.90 \text{ fm}$ into (13), we obtain

$$\frac{g_{KNA}}{\sqrt{4\pi}} = -3.77 \quad \text{and} \quad \frac{g_{KN\Sigma}}{\sqrt{4\pi}} = +1.19$$

at $k_k^r = 0$. The results in the range of $0.80 \leq R \leq 1.00 \text{ fm}$ are listed in Table 1. It is shown that the vector meson contributions are larger than the pseudoscalar meson contri-

Table 1. The KNA and $KN\Sigma$ coupling constants in the range of $0.80 \leq R \leq 1.00 \text{ fm}$. The values in parentheses are for the $g_{KN\Sigma}$. Here, g_v is determined by the renormalized πNN coupling constant $g_{\pi NN}^2/4\pi = 14.3$ for each bag radius

diagrams	the bag radius R (the gauge coupling constant g_v)		
	0.80 fm(5.07)	0.90 fm(5.21)	1.00 fm(5.34)
(3a)	-2.69(0.52)	-2.69(0.52)	-2.69(0.52)
(3b)	-0.27(0.12)	-0.24(0.11)	-0.21(0.10)
(3c)	-0.11(0.04)	-0.09(0.03)	-0.08(0.03)
(3d)	-0.21(0.08)	-0.19(0.07)	-0.17(0.06)
(3e)	-0.14(0.09)	-0.13(0.08)	-0.12(0.08)
(3f)	-0.46(0.39)	-0.43(0.38)	-0.40(0.36)
sum	-3.88(1.24)	-3.77(1.19)	-3.67(1.15)

Table 2. The KNA and $KN\Sigma$ coupling constants. Set I and II are the results extracted from the analyses of the kaon photoproduction. III and IV are the results extracted from the analyses of the kaon-nucleon scattering. V is the Skyrme Model predictions, and VI is a QCD sum rule predictions including the $SU(3)$ symmetry breaking effects. VII is the present calculations from the $SU(3)$ CBMVM at the bag radius $R = 0.90 fm$. The signs of III and IV are not determined

	I[2]	II[29]	III[30]	IV[31]	V[32]	VI[33]	VII(0.90 fm)
$g_{KNA}/\sqrt{4\pi}$	-4.17 ± 0.75	-3.16 ± 0.01	3.73	3.53	-2.17	-2.76	-3.77
$g_{KN\Sigma}/\sqrt{4\pi}$	$+1.18 \pm 0.66$	$+0.91 \pm 0.10$	1.82	1.53	+0.76	+0.44	+1.19

Contributions. Particularly, the importance of the Wess-Zumino term is obvious as listed in (3f) of Table 1. The values extracted from the kaon photoproduction [2,29] and kaon-nucleon scattering experiments [30,31] are listed in Table 2 with our value and other theoretical predictions. Our values for g_{KNA} and $g_{KN\Sigma}$ are existing within the experimental limits of the phenomenological values extracted from the kaon photoproduction of [2]. Compared with the values extracted from the kaon-nucleon scattering, our g_{KNA} is very close to the extracted values while our $g_{KN\Sigma}$ falls short of the extracted those. It should be stressed that our results support the values extracted from the phenomenological analyses, although they have large uncertainties due to the simultaneous determinations of many unknown coupling constants. In Fig. 4, we show the numerical results for the hadronic form factors $g_{\pi NN}(k_\pi)$, $g_{\pi N\Delta}(k_\pi)$, $g_{KNA}(k_k)$ and $g_{KN\Sigma}(k_k)$, where we use the bag radius $R = 0.90 fm$. We can see that the $KN\Sigma$ form factor falls down considerably faster than the other form factors. The reason is that the meson contributions are relatively large while the bare quark contribution of the Feynman diagram (3a) is very small compared with the other form factors. Notice that the meson contribution falls down considerably faster than the quark contribution as shown in Fig. 2.

5 Conclusion

Our calculations based on the $SU(3)$ chiral bag model with vector mesons contain two parameters, i.e. the bag radius R and the quark-vector meson coupling constant g_v . However, g_v is determined by the renormalized πNN coupling constant $g_{\pi NN}^2/(4\pi) = 14.3$ through the relation given in (10). Accordingly, it can have a different value if value of R varies. In this sense, we have (R, g_v) as a free parametric set. Using the parametric values in the range of $(0.80 \leq R \leq 1.00 fm, 5.07 \leq g_v \leq 5.34)$, we obtain the value of the KNA and $KN\Sigma$ coupling constants as follows

$$\begin{aligned} -3.88 &\leq g_{KNA} \leq -3.67, \\ +1.24 &\geq g_{KN\Sigma} \geq +1.15. \end{aligned}$$

These values are considerably close to the phenomenological those extracted from the kaon photoproduction and the kaon-nucleon scattering, while other theoretical predictions fall short of the experimental limits. The reason of these enhancements is actually the point that we take

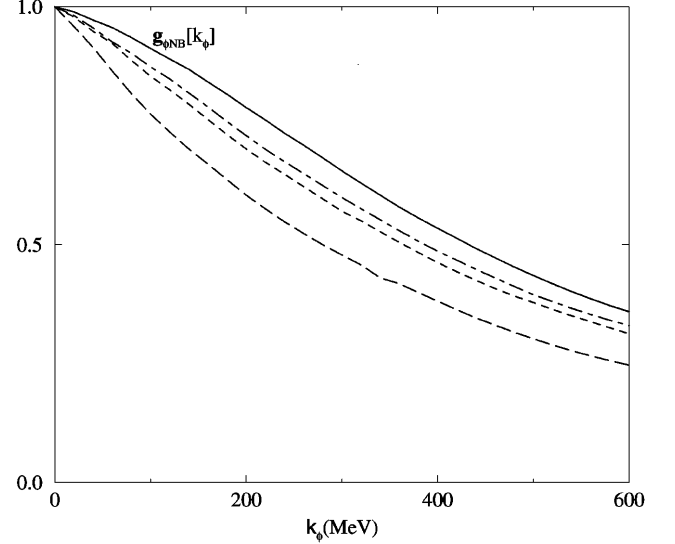


Fig. 4. The renormalized πNN , $\pi N\Delta$, KNA and $KN\Sigma$ form factors. The solid, short dashed, dot-dashed and long dashed curves represent πNN , $\pi N\Delta$, KNA and $KN\Sigma$ form factors, respectively, at the bag radius $R = 0.90 fm$

into account meson ($\pi, K, \rho, \omega, K^*$) field effects, and the Wess-Zumino term. It is again stressed that our results support the values obtained from the phenomenological analyses.

This work was also supported by the Korean Ministry of Education (Grant no. 98-015-D00061 and 98-001-D00249) and Korean Science and Engineering Foundation (Grant no. 961-0204-018-2 and 976-0200-002-2). One of us (M. T. Jeong) was supported by the Dongshin University research grants in 1998.

References

1. R. Buettgen et al., Nucl. Phys. **A506**, 586 (1990)
2. R. A. Adelseck and B. Saghai, Phys. Rev. **C42**, 108(1990); **C45**, 2030 (1992)
3. R. A. Adelseck, C. Benhold and L. E. Wright, Phys. Rev. **C32**, 1681 (1985)
4. H. Thom, Phys. Rev. **25**, 151 (1966)
5. H. Tanabe, M. Kohno and C. Bennhold, Phys. Rev. **C39**, 741 (1989)
6. DeGrand, R. L. Jaffe, K. Johnson, and J. Kiskis, Phys. Rev. **D12**, 2060 (1975)
7. R. Friedberg and T. D. Lee, Phys. Rev. **D15**, 1694 (1977)

8. Adkins, C. R. Nappi, and E. Witten, Nucl. Phys. **B228**, 552 (1983)
9. R. T. Cahill and C. D. Roberts, Phys. Rev. **D32**, 2419 (1985)
10. M. C. Birse and M. K. Banerjee, Phys. Rev. **D31**, 118 (1985)
11. S. Kahana and G. Ripka, Nucl. Phys. **A429**, 462 (1984)
12. R. Seki and S. Ohta, Nucl. Phys. **437**, 541 (1985)
13. G. Kalbermann and J. M. Eisenberg, Phys. Rev. **D28**, 71 (1983)
14. S. Theberge and A. W. Thomas, Nucl. Phys. **A393**, 252 (1983)
15. G. S. Adkins and C. R. Nappi, Phys. Lett. **B137**, 251 (1984)
16. V. Vento, Phys. Lett. **B107**, 5 (1981)
17. M. Araki, Phys. Rev. **C35**, 1954 (1987)
18. Y. J. Oh, K. J. Kong and Il-Tong Cheon, Phys. Rev. **D37**, 2570 (1988); S. Lee, K. J. Kong and Il-Tong Cheon, Phys. Lett. **202**, 21 (1988)
19. M. T. Jeong and Il-T. Cheon, Phys. Rev. **D43**, 3725 (1991)
20. U.-G. Meissner and N. Kaiser, Z. Phys. **A325**, 267 (1986)
21. K. Kawarabayashi and M. Suzuki, Phys. Rev. Lett. **16**, 225 (1966); Riazuddin and Fayyazuddin, Phys. Rev. **158**, 1447 (1967)
22. J. J. Sakurai, **Currents and Mesons** (The Univ. Chicago Press, Chicago, 1969)
23. I. Blomqvist and J. M. Laget, Nucl. Phys. **A280**, 405 (1977); J. M. Laget, Nucl. Phys. **A481**, 765 (1988)
24. C. Schutz, J. Haidenbauer and K. Holinde, Phys. Rev. **C54**, 1561 (1996)
25. C. Schutz, J. W. Durso, K. Holinde and J. Speth, Phys. Rev. **C49**, 2671 (1994)
26. T. Kitagaki, H. Yuta, S. Tanaka, A. Yamaguchi, K. Abe, K. Hasegawa, K. Tamai, H. Sagawa, K. Akatsuka, K. Funo, K. tamae, M. Higuchi, M. Sato, S. A. Kahn, M. J. Murtagh, R. B. Palmer, N. P. Smios and M. Tanaka, Phys. Rev. **D42**, 1331 (1990)
27. J. J. J. Kokkedee, **The Quark Model** (W. A. Benjamin Inc., New York, 1969)
28. Particle Data Groups, Phys. Rev. **D45**, Part 2 (1992)
29. J.-C. David, C. Fayard, G. H. Lamot and B. Saghai, Phys. Rev. **C53**, 2613 (1996)
30. A. D. Martin, Nucl. Phys. **B179**, 33 (1981)
31. J. Antolin, Z. Phys. **C31** 417 (1986)
32. C. Gobbi, D. O. Riska and N. N. Scoccola, Nucl. Phys. **A554**, 671 (1992)
33. S. Choe, M. K. Cheoun and S. H. Lee, Phys. Rev. **53**, 1363 (1996)